Advances in Molecular Biology (1-2): 17-26, 2009
İstanbul Kültür University, Printed in Turkey
www.advmolbiol.org

Spatial arrangement of the animal male germ cell genome: IV. Radiation-induced locus-specific translocations (2;3) and large-scale organization of *Drosophila* sperm nucleus

Igor D. Alexandrov[1]*, Victor A. Stepanenko[2], Margarita V. Alexandrova[1], Svetlana V. Korablinova[1] and Larisa N. Korovina[1]

[1] Dzhelepov Laboratory of Nuclear Problems, Joint Institute for Nuclear Research, 141980 Dubna, Moscow Region, Russia

[2] Laboratory of Information Technologies, Joint Institute for Nuclear Research

Abstract

At the previous papers (Alexandrov *et al*., 2007b, 2008), the specific megarosette-loop organization (but not polar-linear Rabl-configuration) of major haploid autosome 2 in *Drosophila* sperm nucleus has been proposed and experimentally substantiated by analysis of radiation-induced locus-specific inversions showing highly non-randomly distribution of the second inversion breakpoints over the entire autosome. We have speculated that spatial organization of the other major chromosomes in *Drosophila* sperm nucleus must be the same. To test this expectations, the nature and frequency of radiation-induced interchromosomal exchanges (reciprocal translocations) between autosomes 2 and 3 with the first breaks invariantly associated with the same genetic loci (*black* or *vestigial*) on the autosome 2 were studied and, at once, the distribution patterns of the second translocation breakpoints over the entire autosome 3 were detected. Analysis of 23 translocations scored has shown that both *black* and *vestigial* loci highly non-randomly interact with certain, including pericentromeric heterochromatin, "hot" areas of autosome 3. Surprisingly, positioning of these areas found to be co-linear with that of "hot" areas for inversion breakpoints on the autosome 2 if both euchromatic arms and pericentromeric heterochromatic regions of two major autosomes arrange in parallel to each other, showing thereby that spatial organization of both autosomes 2 and 3 goes on concurrently with space and time. Using these data, 2D and 3D models of spatial arrangement of autosome 3 in *Drosophila* haploid sperm nucleus were constructed the principle features of which found to be well consistent with the megarosette-loop configuration proposed for the second chromosome. Independent reciprocal translocations (2;3) scored in the genome of the eight radiation-induced "point" *black* or *vestigial* mutants turned out to have the breakpoints within the autosomes 2 and 3 areas proximity of which is predetermined by the megarosette-loop configuration of these major chromosomes. These results show that approaches of the classical radiation cytogenetics and genetics employed in our genomic investigations may be useful strategy to assist in the elucidation of the other conceptual point in the dynamics of sperm nucleus as a self-organizing system, namely, whether the chromatic protein remodeling (histon -to- protamine transition) in late spermatids is coupled with the structural reorganization of

* Correspondence author:
Dzhelepov Laboratory of Nuclear Problems, Joint Institute for Nuclear Research, 141980 Dubna, Moscow Region, Russia E-mail: igdon@jinr.ru

Received: September, 07, 2009, Accepted: November, 11, 2009.

primary polar-linear Rabl's state of chromosomes in the early post-meiotic spermatids into the compact megarosette-loop structures in the fully mature spermatozoa.

Key words: Radiation, translocations, megarosette-loop configuration of haploid chromosomes, self-organization, sperm genome, *Drosophila*

Introduction

Recently using *Drosophila melanogaster* as a key model organism in current animal biology and genetics (Bier, 2005) as well as the approaches of classical radiation genetics and cytogenetics for study of induction patterns of locus-specific inversions we have provided the first important insights into the higher-order organization of a major part (autosome 2) of sperm nucleus in the form of the specific megarosette-loop (but not polar-linear Rabl's) configuration (Alexandrov *et al.*, 2007b, 2008). It might believe that the spatial organization of other major chromosomes in *Drosophila* sperm nucleus must be the same. To test this expectations, the type and rate of radiation-induced locus-specific interchromosomal exchanges (reciprocal translocations) involving autosome 2 and 3 (Ts(2;3)) were studied. Such locus-specific Ts, unlike regularly arising interchanges (2;3) in irradiated *Drosophila* spermatozoa (Eberl *et al.*, 1989), have one (the "first") break invariantly associated with the *black (b)* (almost a middle of 2L arm) or *vestigial (vg)* (a middle of 2R arm) loci on the autosome 2 (T(2;3)*b* and T(2;3)*vg*, respectively) the spatial position of which in 3D megarosette-loop structure of this autosome was certainly identified as closely associated with the pericentromeric heterochromatin (Alexandrov *et al.*, 2008). Therefore, the knowledge of positioning of the second translocation breakpoints in T(2;3)*b* and T(2;3)*vg* permits to detect the chromosomal areas that were spatially close to the gene loci of interest in irradiated sperm nuclei and, thereby, to reconstruct the higher-order loopy organization of this major autosome. To study this issue, the distribution patterns of the second breakpoints over the entire autosome 3 for 8 T(2;3)*b* and 15 T(2;3)*vg* were detected. As the results obtained had shown, both *b* and *vg* gene loci highly non-randomly interact with the certain, including pericentromeric heterochromatin, "hot" areas of autosome 3. Moreover, positioning of these areas found to be co-linear with "hot" areas for inversion breakpoints on the autosome 2 if both autosomes arrange in parallel to each other according to their chromosome map. These findings unequivocally show that the macroarchitecture of autosome 3 in *Drosophila* sperm nucleus in itself principle features is, indeed, similar to that of autosome 2 and, obviously, must have the specific megarosette-loop configuration too.

Table 1. The location of the second translocation breakpoints on the polytene autosome 3 of *D.melanogaster* for γ-ray- and neutron-induced T (2; 3) b (about the "first" breakpoint see text).

No	Code of b translocation	Radiation, dose	The section of autosome 3 with the second translocation breakpoint
1	b91l7	γ-rays, 40 Gy	61D
2	b88g4	n + γ-rays, 20 Gy	62F
3	b88g68	n + γ-rays, 15 Gy	76A
4	b89e12	γ-rays, 40 Gy	79C
5	b79d6	n + γ-rays, 20 Gy	80D
6	b88e88	n + γ-rays, 30 Gy	80D
7	b88g22	n + γ-rays, 30 Gy	87F
8	b85c2	n, 10 Gy	95C

Table 2. The location of the second translocation breakpoints on the polytene autosome 3 of *D.melanogaster* for γ-ray- and neutron-induced T (2; 3) vg (about the "first" breakpoint see text)

No	Code of vg translocation	Radiation, dose	The section of autosome 3 with the second translocation breakpoint
1	vg81a	γ-rays, 40 Gy	64B
2	vg83c	γ-rays, 40 Gy	65F
3	vg88c25	n, 5 Gy	70C
4	vg88d24	γ-rays, 40 Gy	70C
5	vg78b4	γ-rays, 40 Gy	80C
6	vg88f31	n + γ-rays, 20 Gy	80C
7	vg88f58	n + γ-rays, 20 Gy	80D
8	vg87h1	γ-rays, 40 Gy	81F
9	vg88c42	n, 2.5 Gy	81E
10	vg89d1	γ-rays, 40 Gy	83A
11	vg76i1	γ-rays, 40 Gy	84E
12	vg85d2	n, 15 Gy	84F
13	vg88d9	γ-rays, 40 Gy	92C
14	vg67d1	γ-rays, 40 Gy	93E
15	vg79b3	γ-rays, 40 Gy	94A

Table 3. The location of the breakpoints on the polytene chromosomes 2 and 3 of *D.melanogaster* for radiation -induced translocations attendant with the "point" mutations at the b and vg loci mapped at the 34D and 49E autosome 2 sections, respectively.

The "point" locus-specific mutations					
b			vg		
b89e64b	γ, 40 Gy	T(2;3) 47C; 69C	vg88h11,	n + γ, 20 Gy	T(2;3) 39F; 62A
b89e64c	γ, 40 Gy	T(2;3) 55E; 98C	vg87h55	γ, 40 Gy	T(2;3) 41D; 90E
b91l14	γ, 40 Gy	T(2;3) 60A; 65F	vg91l15	γ, 40 Gy	T(2;3) 51C; 89D
			vg87h40	γ, 40 Gy	T(2;3) 56F; 89E
			vg88f21	n + γ, 15 Gy	T(2;3) 60F; 86D

Materials and methods

Random sets of γ-ray- and neutron-induced Ts(2;3)*b* (Table 1) and Ts(2;3)*vg* (Table 2) were obtained at the same experiments in parallel with the *b* and *vg* inversions described earlier (Alexandrov *et al*., 2007a, 2008).The physical as well as biological details of experiments such as *Drosophila* stocks and germ cell irradiated, the sources of radiation (γ-rays of ^{60}Co, fission neutrons, combined action of neutrons and γ-rays), doses and regimes of irradiation can be found elsewhere (Alexandrov, 1984; Alexandrov and Alexandrova, 1989). The results of the cytogenetical analysis of these Ts(2;3) have been presented elsewhere too (Alexandrov and Alexandrova, 1987; 1991). Here, it is note worthy that the precise chromosome location of the second translocation

breakpoints on the autosome 3 was performed by the standard cytological technique for *Drosophila* polytene chromosomes in the mutant (2;3) chromosomes / wild-type chromosomes heterozygous larva and estimated accurately within subsection of the polytene chromosome 3 guided by its classical map under the light microscopy (Lefevre, 1976).

Additionally, random samples of radiation-induced Ts(2;3) with the "first" breakpoints outside of the *b* or *vg* loci were obtained during the same experiments as the interchromosomal exchanges attendant with the "point" mutations at the gene loci of interest (Table 3). The mapping of breakpoints underlying these exchanges was carried out using the same standard cytological technique too.

To test the non-random distribution of the second translocation breakpoints over the entire autosome 3, chi-square analysis was used and $P < 0.05$ was considered as significant.

Results and discussion

The Ts(2;3)*b* and Ts(2;3)*vg*

According to dataset of our large-scale radiation experiments on the mutation induction at the *b* and *vg* gene loci, both Ts(2;3)*b* and Ts(2;3)*vg* are regularly induced in *Drosophila* sperm nuclei irradiated (Alexandrov *et al.*, 1997). Thereby, the induction rate of Ts(2;3)*b* is almost twice as small as that of Ts(2;3)*vg*. Indeed, only 8 out of 189 (4.2 %) γ-ray- or neutron-induced *b* mutants scored and precisely analysed were associated with translocations in question (Table 1) whereas as much as 15 out of 198 (7.6 %) radiation-induced *vg* mutants isolated during the same experiments were based on such translocations (Table 2).

Close inspection of the tabulated data on positioning of the second translocation breakpoints over a length of autosome 3 permits to note that 23 (in totality) breakpoints are highly non-randomly distributed over 40 sections of this autosome affecting singly or repeatedly only 9 regions among them ($\chi^2 = 99.53$; d. f. = 4; $P < 0.005$). Amid affected regions, pericentromeric heterochromatin (sections 79-81) of autosome 3 found to be the most "hot" chromosome area with which both the *b* and *vg* regions of autosome 2 interact more often (8 cases out of 23 or 34.8 %). Taking into account the fact that both genes in question are preferentially positioned too in spatial proximity relative to pericentromeric heterochromatin of their own autosome to give rise the radiation-induced inversions (Alexandrov *et al.*, 2007a, 2008) it is felt that pericentromeric heterochromatin areas of both autosomes 2 and 3 are organized on genome-wide scale in sperm nucleus as an unified heterochromatic compartment.

In parallel with heterochromatin, it is observed several specific euchromatic "hot" areas of autosome 3 with which both gene *b* and *vg* regions interact repeatedly, such as adjacent 61-62 sections (telomeric end of 3L arm) for the gene locus *b* (Table 1) and adjacent sections 64-65 (subtelomeric region of 3L arm), section 70 (a middle of 3L arm), adjacent sections 83-84 (pericentromeric area of 3R arm), and contiguous sections 92-94 (almost a middle of 3R arm) for the gene locus *vg* (Table 2). The rest 3 Ts(2;3)*b* are based on the scarce alternative interaction of the *b* region with 76 (close to heterochromatin), 87 or 95 (middle positions in 3R arm) sections.

Thus, at least eight euchromatin areas of autosome 3 (in twos in 3L and 3R arms for the *b* and *vg* loci) show the spatial proximity relative to the two autosome 2 gene loci under study. The integration of euchromatic areas listed in the neighbourhood of heterochromatic compartment of sperm nucleus generates the higher-order arrangement of autosome 3 in the form of, at least, eight-looped rosette-like structure. The sizes of expected giant loops in such configuration should comprise of 4, 10, 15 and 18 chromosome sections in 3L arm and of 3, 6, 12 and 14 sections in 3R arm reading from autosome 3 heterochromatin to telomeric ends or 4.8, 12, 18 and 21.6 as well as 3.6, 7.2, 14.4 and 16.8 Mb of DNA, respectively, taking into account the fact that each section contains on average about 1.2 million pairs of DNA bases (Mb) (Adams *et al.*, 2000).

The putative rosette-loop configuration of autosome 3 must have topological properties much

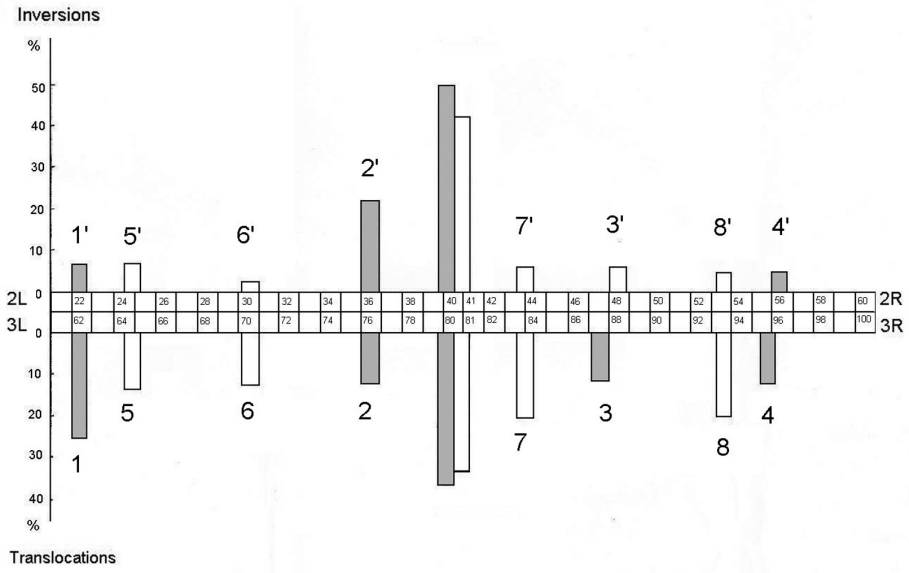

Figure 1. The relative rate and location of the second inversion (top) and translocation (bottom) breakpoints over the entire autosomes 2 and 3, respectively, for the *black* (□) and *vestigial* (□) exchanges induced by different quality radiation in *Drosophila* mature spermatozoa (for details see text). The numbers 1, 2, 3, 4 and 5, 6, 7, 8 denote the autosome 3 sections with breakpoints for Ts(2,3)*b* and Ts(2,3)*vg*, respectively, whereas the number 1', 2', 3', 4' and 5' , 6', 7', 8' denote the relevant competitive sections of autosome 2 with breakpoints for Ins(2)*b* and Ins(2)*vg,* accordingly.

like those of autosome 2. This notion is independently confirmed by the comparative analysis of positioning of both translocation (autosome 3) and inversion (autosome 2) second breakpoints (Figure 1). As seen, if both metacentric autosomes are arranged in parallel to each other according to their standard section maps, there is one-to-one correspondence between positioning of all five translocation breakpoint regions on autosome 3 (64-65, 70, 80-81: heterochromatin, 83-84 and 92-94) and that of relevant inversion breakpoint regions on autosome 2 (24-25, 30, 40-41: heterochromatin, 43-44 and 52-54) for the *vg* exchanges as well as for the b exchanges (61-62, 76, 79-80: heterochromatic region, and 95 on autosome 3 and 22, 35-36, 40-41: heterochromatin, and 56 on autosome 2) (for relevant *vg* and *b* inversions see Alexandrov *et al.*, 2007a; and Alexandrov *et al.*, 2008, respectively).

The excellent correlation in positioning of both translocation and inversion breakpoints listed will not fail to represent the same spatial geometry of two major autosomes in form of megarosette-loop structures. Moreover, both structures are come within short distances of each other at last in the eight chromosomal areas (alongside sections 22 and 62, 24 and 64, 30 and 70, 36 and 76, 40-41 and 80-81, 43-44 and 83-84, 53-54 and 93-94, 56 and 95) (Figure 1) testifying that spatial organization of both autosomes 2 and 3 goes on concurrently with space and time. However, as it can see from Figure 1, these pair-areas are quite different for the gene *b* and *vg* regions interacted with them. These findings enable one to recognize two “sensitive” nuclear microvolumes marked by the gene loci *b* and *vg* together with associated autosome 2 and 3 areas. If so, it is felt that realized probability of radiation-induced interaction of given gene region with one or other neighbouring alternative “partner” (chromosome area) within its own microvolume and, accordingly, the type of exchange observed (translocation or inversion) appear should be determined by chance according to which alternative “partner” will be the most closer to the gene in question in given sperm nucleus at the time of irradiation.

Thus, identification of autosome 3 translocation breakpoints interacting with the two autosome 2 gene loci *b* and *vg* which, in turn, found to be positioned in close spatial proximity relative to the nuclear heretochromatin compartment are creating the basis for 2D as well as 3D computer simulation of global configuration of this autosome. Such models were constructed and just presented below.

2D and 3D models of autosome 3

The large-scale geometry of elementary chromosome 3 fiber in haploid *Drosophila* sperm nucleus was constructed using the basic assumptions and appraches elaborated for 2D and 3D modeling of *Drosophila* auto-some 2 (Alexandrov *et al*., 2007b). Briefly, the following premises of biological meaning were taken for granted: (i) there is a one-to-one correspondence between the classical section banding map of given interphase polytene chromosome in salivary gland somatic cells where the cytological analysis of radiation-induced inversions or translocations have been carried out and the supramolecular (chromomeric) organization of a 30 nm thick elementary fiber of the same chromosome in sperm nucleus irradiated; (ii)totally all affected autosome 3 areas with which the gene loci *b* and *vg* interact to give rise translocations were considered in the modeling due to the fact that the rate of radiation-induced *b* and *vg* translocations is almost four times rare than that of *b* and *vg* inversions induced in sperm nuclei at the same experiments (see Alexandrov *et al.*, 2007a, 2008 and this paper); (iii) heterochromatic compartment encompassing both autosomes 2 and 3 pericentromeric heterochromatin areas is located on the sperm nuclear envelope and considered as a kind of chromosome “anchor” around of which the two gene loci in question and “hot” euchromatin areas interacted with them are grouped.

For purposes of modeling, the Gmax v.1.2 software with some supporting programs were used as it was described earlier (Alexandrov *et al*., 2007b). Among them, method of B splines proved to be particularly promising for modeling of the interphase chromosome fiber (Zaikin *et al.*, 2005). Making a start to construction of the two-dimensional model of autosome 3, the chromosomal positioning of translocation breakpoints interacting with the gene locus *b* have been taken into account in the first place (Table 1). Therewith, the average distances of interaction of chromosome areas with the *b* gene were calculated as quantities which are inversely related to the rates of exchanges observed.

Then, using the consecutive modeling operations described earlier (Alexandrov *et al.*, 2007b), the visual autosome 3 model based on the four its euchromatin areas as markers interacted with the *b* gene region (Table 1, Figure 1) was created (Figure 2A). After that, the independent visual autosome 3 model allowing for the four other translocation breakpoints-markers interacting with the *vg* gene region (Table 2, Figure 1) was constructed (Figure 2B). Finally, both models created were combined with each other (Figure 2C). As seen, the resultant model of elementary autosome 3 fiber based on the eight euchromatin breakpoints-markers corresponds well to the same megarosette-loop configuration as that of autosome 2 fiber described earlier (Alexandrov *et al*., 2007b) testifying on behalf of unitary principle of global arrangement of haploid chromosomes in *Drosophila* sperm nucleus. It is important to note that this arrangement is not consistent with the polar-linear Rabl’s configuration of interphase chromosomes in animal or plant somatic cells.

During construction of three-dimensional model of elementary autosome 3 fiber, the basic modeling steps and operations, such as the method of B splines, setting of reference breakpoints as well as of breakpoint interaction distances or radii of embedded spheres, image and color of chromosome arms, operation of the group selection of objects (Select-by- NAME), illumination of the picture and so on, were used details of which can be found elsewhere (Alexandrov *et al.*, 2007b). The example of 3D model of autosome 3 constructed is pictured in Figure 2D. It needs to note that euchromatin regions without relevant translocation breakpoints were modeled in the relaxed state as in the case of 2D model.

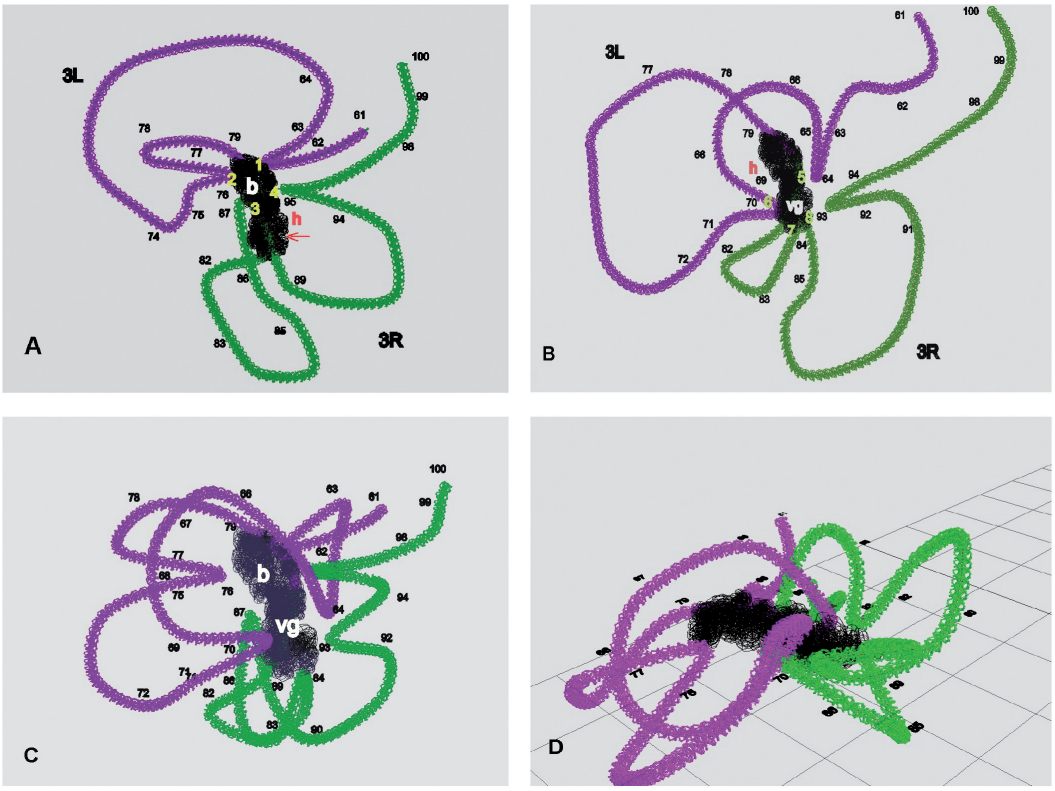

Figure 2. The consecutive steps of 2D modeling of the elementary chromosome 3 fiber macroarchitecture in *Drosophila* sperm nucleus based on the induction pattern of Ts (2;3) *b* (A) and Ts (2;3) *vg* (B); h – heterochromatic compartment; the black number 61; 62 …. 99, 100 denote the relevant sections of autosome 3; *b* and *vg* gene loci mark the putative "sensitive" microvolumes and are positioned in spatial proximity relative to heterochromatic compartment; 3L and 3R indicate the arms of autosome 3; the yellow numbers 1-4 (A) and 5-8 (B) denote the autosome 3 sections with breakpoints for Ts (2;3) *b* and Ts (2;3) *vg*, respectively (see Figure 1). (C) A general 2D model of autosome 3 based on both *b* and *vg* translocation data (symbols are the same as in A and B). (D) An example of a general 3D model of an elementary fiber of autosome 3 in *Drosophila* sperm nucleus. As an idealization, throughout these models all loops without translocation breakpoints are relaxed.

2D model for both autosomes 2 and 3 as an unitary entity

Prior to modeling of large-scale arrangement and interrelation of two major autosomes in *Drosophila* sperm nucleus, the four main our findings above described were first borne in mind: (i) identification of two "sensitive" nuclear microvolumes marked by the autosome 2 gene *b* and *vg* loci; (ii) both microvolumes are positioned in close spatial proximity relative to nuclear heterochromatic compartment; (iii) either of the two microvolumes contain too the specific sets of both autosome 3 and 2 areas with which the *b* and *vg* regions can alternatively interact after irradiation to give rise translocations or inversions; (iv) among all distinct euchromatin areas detected within the microvolumes, the *b* and *vg* regions proved to be most brought into proximity with heterochromatic compartment.

To create the generalized 2D model of two autosomes in question, the same software and

supporting programs were used. As the first step, 2D model based on the eight inversion and translocation breakpoint – markers locations of which are in line over the entire of both autosomes (Figure 1) was constructed. Therewith, the average distances of interaction of each breakpoint- marker with the gene *b* or *vg* region were calculated with regard to the number of interaction observed for both the *b* and *vg* inversions and translocations as well (Alexandrov *et al.*, 2007a, 2008, this paper). A visual (colored) 2D model constructed on the basis of this approaches is depicted in Figure 3A. In this case, both autosomes supposed to be arranged in parallel to each other over the entire their stretches. The use of extra inversion breakpoint-markers identified for the vg inversions (sections 21, 35, 50 and 59-60 on autosome 2) (Alexandrov *et al.*, 2007a) gives rise to more compact generalized 2D model of both autosomes in which formerly relaxed euchromatic areas and freely lying telomeric ends turn out quite near with the vg gene locus and heterochromatic compartment (Figure 3B).

Non-b or vg-specific translocations

The formerly (in 2D and 3D models) relaxed giant loops of autosomes under study should be evidently arranged more compact in the native sperm nucleus creating the premises for radiation-induced interaction of intralooped chromatin areas and, thus, for arising of non-*b*- or *vg*-specific translocations with the characteristic patterns guided by the global megarosette-loop configuration of the entire autosomes. It is important now to recall that in this configuration the both autosomes 2 and 3 are looped and arranged co-linear in the nuclear space showing the spatial proximity of the same euchromatin regions along their standard chromosome maps (Figure 1). Taking into account these specific features of higher-order organization of both autosomes in *Drosophila* sperm nucleus, it is of interest and important to know as to whether the induction patterns of radiation-induced independent translocations scoring in the genome of the "point" *b* and *vg* mutants were actually predetermined by specific chromosome macroarchitecture proposed.

The analysis of 8 Ts(2;3) occasionally arisen in genome of 3 *b* and 5 *vg* "point" mutants (Table 3) shows that 5 out of 8 (62.5 %) these translocations, namely, Ts(2;3) *b* No1 and 3 as well as Ts(2;3) *vg* No 2,3 and 4 are based on interaction of chromosome areas which, according to model, are located within microvolume marked by the gene *vg* locus and were

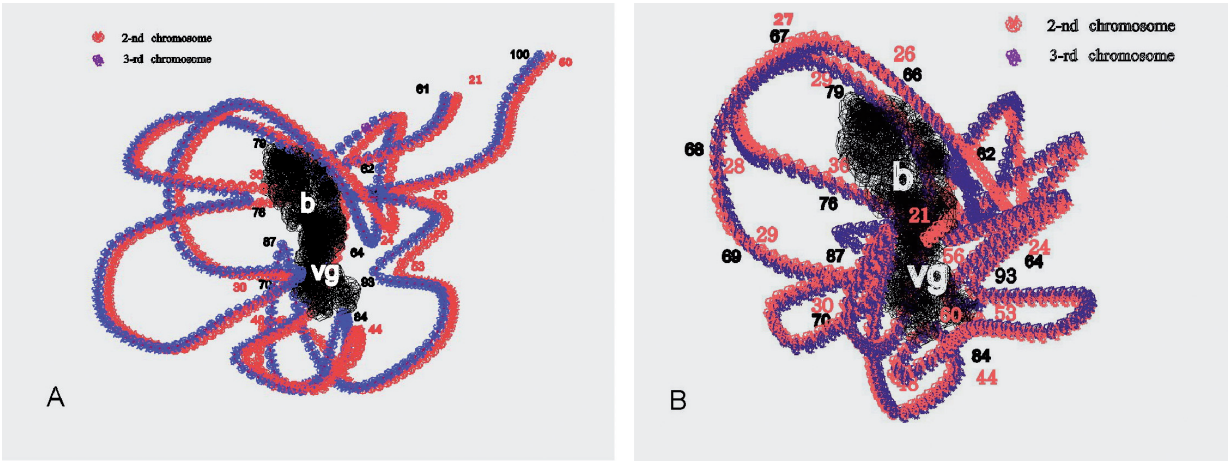

Figure 3. An example of a general 2D model for both autosomes 2 and 3 as an unitary entity based on (A) eight inversion and translocation breakpoints positions of which are in line over the entire of both autosomes (details see Figure 1) and (B) the same 2D model with extra inversion breakpoints (see text). Symbols are the same as in Figure 2.

already involved into the *vg* exchanges as such or as an adjacent regions. The rest Ts(2;3) may be expected due to proximity of relevant chromosome areas determined by the model and co-linear arrangement of autosomes in question. Therefore, the independent occurrence of translocations considered is reasonably expected within the framework of the model suggested.

Moreover, a new independent and strong evidences in support of our model may really provide a close inspection of the available data reported elsewhere (Eberl *et al.*, 1989). It is quite obvious from the careful examination of these data that many (64 out of 81 or 79.0 %) of γ-ray-induced rearrangements scored and characterized precisely cytologically as interchanges involving the major autosomes 2 and 3 in *Drosophila melanogaster* spermatozoa have resulted from interaction of breakpoints located within the chromosome areas proximity of which appears to be well predicted by the model suggested taking into consideration all its specific features above pointed out. The rest Ts(2;3) may give evidence of more compact and multilooped organization of haploid chromosomes than it follows from the model created, on the one hand, or of the biological variability, on the other hand, or both.

Interestingly and significantly enough that, according to the data of classical radiation genetics of *D. melanogaster*, many of radiation-induced mutations at the sex-linked *yellow* (*y*) and *scute (sc)* loci immediately adjacent to the telomere of this large X chromosome shown to be associated with inversion or translocation breaks the second breakpoints of which are repeatedly located within the heterochromatin (y^{3P}, y^{v1}, sc^{s1}, sc^{s4}, sc^{8}, $sc^{260\text{-}18}$ etc.) or in the middle areas of their own X (y^{s}) chromosome as well as of both autosomes ($y^{260\text{-}13}$, $sc^{260\text{-}15}$, $sc^{260\text{-}17}$) and in subtelomeric regions of 2R (sc^{s2}) or 3L (sc^{i4}, sc^{k3}, $sc^{260\text{-}20}$) arms of autosomes too (Lidsley and Greel, 1968). These data and our results show that telomeric, middle and heterochromatic regions of all major chromosomes in *Drosophila* mature sperm nucleus are spatially close to each other forming the same megarosette-loop configurations.

Maturing sperm nucleus as a self-organizing system

Complete transformation of linear-polar structure of large metacentric haploid chromosomes in *Drosophila* early postmeiotic spermatids into the unusual and unique megarosette-loop configuration in the motile mature sperms characterizes the nucleus of differentiating spermatids as a highly dynamic entity. Taken together, these structural changes as well as a specific morphogenetic and synthetic processes touching on the cytoplasmic organelles and chromosomal histone (chromatin remodeling or histone-to protamine transition) in sperm maturation (Kimmins and Sassone-Corci, 2005) provide the basis for concept that the maturing sperm nucleus may be a self-organizing system as satisfying its major principle, namely, the availability of "the high dynamic content and a relative promiscuity of interactions amongst components" (Misteli, 2005).

An understanding of the maturing sperm nucleus as a self-organizing system raises a broad range of issues relating to the spatiotemporal pattern of higher-order chromosome reorganization and its molecular mechanisms (the meaning of DNA sequences, forces guiding this reorganization etc.). The approaches to study the latter issues are based on using of a complex of modern molecular techniques that are too costly and extended in time. To investigate the first issue and to test our premise that higher-order chromosome reorganization is coupled with the chromatic protein remodeling in late spermatids. The approaches of the classical radiation genetics and cytogenetics employed in our genomic studies and the results of which have been presented at four consecutive papers in this journal (Alexandrov *et al.*, 2007a,b, 2008, this volume) presumed may be the most promise.

Acknowledgement

We are grateful to Alexandr L. Karpovsky for technical assistance.

References

Adams MD, Celniker SE, Holt RA *et al.* The genome sequence of *Drosophila melanogaste*r. *Science*. 287: 2185-2195, 2000.

Alexandrov ID. Quality and frequency patterns of γ- and neutron-induced visible mutations in *Drosophila* spermatozoa. *Mutation Research*, 127: 123-127, 1984

Alexandrov ID, Alexandrova MV. Genetics and cytogenetics of the *vestigial* mutations induced by gamma-rays, ^{252}Cf and fission neutrons. *Drosophila Inform. Service*. 66: 185-187, 1987

Alexandrov ID and Alexandrova MV. Spectrum and frequency of inheritable mutations after combined action of neutrons and γ-rays. In "Neutrons and Hard-Charged Particles in Biology and Medicine". (Rus.) Obninsk. 6-17. 1989

Alexandrov ID and Alexandrova MV. The genetic and cytogenetic boundaries of the radiation induced rearrangements scored as lethal *black* mutations in *D. melanogaster*. *Drosophila Inform. Service*. 70: 16-19, 1991.

Alexandrov ID, Zakharov IA and Alexandrova MV. The Moscow Regional *Drosophila melanogaster* Stock Center. *Drosophila Inform. Service*. 80: 109-130, 1997

Alexandrov ID, Alexandrova MV, Korablinova SV and Korovina LN. Spatial arrangement of the animal germ cell genome: I. Non-random pattern of radiation-induced inversions involving the vestigial region in autosome 2 of *Drosophila melanogaster*. *Advances in Molecular Biology* (1): 23-29, 2007a.

Alexandrov ID, Stepanenko VA and Alexandrova MV.39 spatial arrangement of the animal male germ cell genome: II. 2D-3D simulation and visualization of spatial configuration of major chromosome 2 in *Drosophila* sperm. *Advances in Molecular Biology* (1): 71-77. 2007b.

Alexandrov ID, Alexandrova MV, Stepanenko VA, Korablinova SV, Korovina LN and Stetsenko SG. Spatial arrangement of animal male germ cell genome: III. A new experimental evidences in support of the megarosette-loop model of spatial organization of chromosomes in *Drosophila* sperm genome. *Advances in Molecular Biology*. 2: 23-30. 2008.

Bier IE. *Drosophila*, the golden hug, emerges as a tool for human genetics. *Nat. Rev. Genet.* 6: 9-23. 2005.

Eberl DF, Hiliker AJ, Sharp CB and Trusis-Coulter SN. Further observations on the nature of radiation-induced chromosomal interchanges recovered from *Drosophila* sperm. *Genome,* 32:5, 847-855, 1989.

Kimmins S, Sassone-Corci P. Chromatin remodeling and epigenetic features of germ cells. *Nature*, 434: 583-589, 2005.

Lefevre GJr. A photographic representation and interpretation of the polytene chromosomes of *Drosophila melanogaster* salivary glands. In: The Genetic and Biology of Drosophila. Edited by M. Ashburner, E. Novitski. London: Acad. Press. V.1a, p.31-66, 1976

Lindsley DL and Greel EH. Genetic variations of *Drosophila melanogaster*. Carnegie Inst. of Washington Pabl., No 627, 471 pp, 1968.

Misteli T. Concepts in nuclear architecture. *BioEssays* 27: 477-487, 2005

Zaikin NS, Korenkov VV and Stepanenko VA. 3D modeling and visualization of subjects on the base of GMAX program. Annual Report 2005, Joint Inst. Nucl.Res., Lab. Inform. Technol. (Eds. Gh.Adam, VV Ivanov, TA Strizh), Dubna, Russia, p.160-162, 2005